

Genetic basis of ecologically relevant body shape variation among four genera of cichlid fishes

Leah DeLorenzo¹  | Destiny Mathews¹ | A. Allyson Brandon¹ | Mansi Joglekar¹ |
 Aldo Carmona Baez²  | Emily C. Moore^{2,3}  | Patrick J. Cicotto^{2,4} |
 Natalie B. Roberts² | Reade B. Roberts²  | Kara E. Powder¹ 

¹Department of Biological Sciences,
Clemson University, Clemson, South
Carolina, USA

²Department of Biological Sciences, and
Genetics and Genomics Academy, North
Carolina State University, Raleigh, North
Carolina, USA

³Department of Biological Sciences,
University of Montana, Missoula,
Montana, USA

⁴Department of Biology, Warren Wilson
College, Swannanoa, North Carolina, USA

Correspondence

Kara E. Powder, Department of Biological
Sciences, Clemson University, 055A Life
Science Facility, 190 Collings Street,
Clemson, SC 29634, USA.

Email: kpowder@clemson.edu

Funding information

Arnold and Mabel Beckman Foundation;
National Institute of Dental and
Craniofacial Research, Grant/Award
Number: R15DE029945; National
Institute of General Medical Sciences,
Grant/Award Number: P20GM121342;
National Science Foundation, Grant/
Award Number: #1942178 and IOS-
1456765

Handling Editor: Paul A. Hohenlohe

Abstract

Divergence in body shape is one of the most widespread and repeated patterns of morphological variation in fishes and is associated with habitat specification and swimming mechanics. Such ecological diversification is the first stage of the explosive adaptive radiation of cichlid fishes in the East African Rift Lakes. We use two hybrid crosses of cichlids (*Metriaclima* sp. \times *Aulonocara* sp. and *Labidochromis* sp. \times *Labeotropheus* sp., >975 animals total) to determine the genetic basis of body shape diversification that is similar to benthic-pelagic divergence across fishes. Using a series of both linear and geometric shape measurements, we identified 34 quantitative trait loci (QTL) that underlie various aspects of body shape variation. These QTL are spread throughout the genome, each explaining 3.2–8.6% of phenotypic variation, and are largely modular. Further, QTL are distinct both between these two crosses of Lake Malawi cichlids and compared to previously identified QTL for body shape in fishes such as sticklebacks. We find that body shape is controlled by many genes of small effect. In all, we find that convergent body shape phenotypes commonly observed across fish clades are most likely due to distinct genetic and molecular mechanisms.

KEY WORDS

adaptation, Cichlidae, fish diversification, quantitative trait loci

1 | INTRODUCTION

Body shape variation is common across all vertebrates and has important consequences for an animal's ecology, locomotion, thermodynamics and even speciation (Arnold, 1983, 1992; Coyne & Orr, 2004; Friedman et al., 2021; Ruff, 1991; Schlüter, 1996, 2000; Smith et al., 2015). A major axis of this morphological

variation is body elongation, which occurs within reptiles (Bergmann & Irschick, 2012; Losos, 2009; Wiens & Slingluff, 2001), carnivorous mammals (Law, 2019, 2021) and fishes (Friedman et al., 2020; Price et al., 2019; Ward & Mehta, 2010).

One of the most widespread and repeated patterns of eco-morphological variation within both marine and freshwater fishes is variation in body shape and fin position, often associated with

This is an open access article under the terms of the [Creative Commons Attribution-NonCommercial](#) License, which permits use, distribution and reproduction in any medium, provided the original work is properly cited and is not used for commercial purposes.

© 2023 The Authors. *Molecular Ecology* published by John Wiley & Sons Ltd.

divergence along the benthic-pelagic axis (Burns & Sidlauskas, 2018; Hulsey et al., 2013; Kusche et al., 2014; Muschick et al., 2012; Price et al., 2019; Ribeiro et al., 2018; Robinson & Wilson, 1994; Rogers & Jamniczky, 2014; Schlüter, 1996; Walker, 1997; Willacker et al., 2010). This morphological divergence occurs similarly in ancient fish radiations (Ribeiro et al., 2018), at the macroevolutionary level (Claverie & Wainwright, 2014; Friedman et al., 2020; Larouche et al., 2020; Price et al., 2019) and repeatedly at the microevolutionary level (Brachmann et al., 2021; Hatfield & Schlüter, 1999; Walker, 1997).

Body shape and fin placement dictate how fishes navigate their ecological niches. For instance, fishes that live in environments with variation in structure and water flow generally have a deeper, more stout body thought to be adaptive for increased manoeuvrability and body rotation (Webb, 1982, 1984). A deeper caudal peduncle and more posterior placement of the anal and dorsal fins enable fishes to have fast propulsion as they move, change direction and adjust to varied water flow patterns in their complex habitats (Koehl, 1984; Webb, 1982). This body variation can be coordinated with changes in head shape, namely a shorter head region (Cooper et al., 2010). Alternatively, a narrow fusiform body shape is often associated with larger head proportions and is thought to enhance the performance of sustained swimming ('cruising') while minimizing drag in open water (Cooper et al., 2010; Friedman et al., 2020; Raffini et al., 2020; Schlüter & McPhail, 1992; Webb, 1982, 1984).

We examine the genetic basis of body shape variation using a textbook example of adaptive radiation, cichlid fishes. Within cichlids, ecological divergence is critical to their adaptive radiation (Kocher, 2004; Streelman & Danley, 2003) and occurs repeatedly, independently and convergently in three expansive radiations in East African Rift Lakes (Cooper et al., 2010; Hulsey et al., 2013, 2018; Muschick et al., 2012; Ruber & Adams, 2001) as well as smaller radiations within New World crater lakes (Elmer et al., 2010; Franchini et al., 2014; Kusche et al., 2014). Notably, hybrids among different cichlid species or even genera can be produced in the laboratory, enabling quantitative trait loci (QTL) mapping of phenotypic variation (Powder & Albertson, 2016).

We therefore capitalized on the genetics and extensive phenotypic variation of cichlids to investigate the genetic basis of body shape divergence, a major axis of fish diversification. First, we determined the genetics of body shape within each cross, using species at varying points along a body shape morphological continuum. This allows us to examine if different aspects of body shape variation have similar or distinct regulatory bases, which has important implications for the evolution of these traits. Then, we compare if the genetic intervals and mechanisms of divergence are similar between the two hybrid crosses. If so, this would indicate a shared molecular control as animals evolve towards distinct body shapes. Second, we assess the genetic architecture of body shape evolution in cichlids. We ask if there are many genetic loci that each contribute small effects or few regions with large effects that regulate body shape. Body shape variation within stickleback fishes has been attributed to a combination of a few QTL with large effects and many QTL with small effects (Albert et al., 2008; Liu et al., 2014; Yang et al., 2016). Further,

QTL for body shape and other morphological features in sticklebacks have been suggested to cluster on certain chromosomes, and these 'supergene' regions can influence coordinated changes in phenotype (Albert et al., 2008; Liu et al., 2014; Miller et al., 2014). Finally, we ask if this common and predictable morphological trajectory in fishes has a predictable genetic basis by comparing QTL for body shape across multiple fish species. In other words, we determine if there is parallelism in the genetics of body shape variation to accompany convergent morphologies among fishes. To accomplish these goals, we utilized two hybrid crosses of Lake Malawi cichlids, quantifying a suite of linear and geometric measures of body shape. We use QTL mapping to identify the genetic bases of these traits, which we then compare among traits, between crosses and to studies in other non-cichlid fishes. Together, these data provide insights into the genetic control of a major ecological and morphological divergence in animals.

2 | MATERIALS AND METHODS

2.1 | Animals and pedigree

All animal care was conducted under approved IACUC protocol 14-101-O at North Carolina State University. Four species of Lake Malawi cichlids were used: *Aulonocara koningsi*, *Metriaclima mbenji*, *Labidochromis caeruleus* and *Labeotropheus trewavasae*, hereafter referred to by the genus name. These fish have varied ecological specifications and swimming mechanics. *Aulonocara* lives within an open, sandy region, away from the complex rocky habitat of the other species used here, and forages by cruising over the open sand. The *Labidochromis* species studied here lives in and around rocky habitats, but is non-territorial and swims continuously, darting among rocks in search of invertebrate prey. *Metriaclima* is a generalist rock-dwelling fish that often enters the water column, and *Labeotropheus* represents a more specialized rock-dwelling morphology and behaviour (Cooper et al., 2010; Konings, 2016). Two hybrid crosses of these species were generated. The first cross came from a single *Metriaclima* female crossed to two *Aulonocara* males; the inclusion of the second grandsire was inadvertent and resulted from an unexpected fertilization event in these species with external fertilization (see *ddRAD-sequencing* section for how this was addressed during genotyping). The second cross came from a single *Labidochromis* female crossed to a single *Labeotropheus* male. Thus, both crosses feature a fish that dominantly 'cruises', a pelagic swimming tactic, versus a more benthic species. For each cross, a single F_1 family was generated and subsequently in-crossed to produce F_2 hybrid mapping populations. F_2 families were raised in density-controlled aquaria with standardized measured feedings until 5 months of age for analysis. Fish were anaesthetized with buffered 100 mg/L MS-222 for all photographs. Whole fish photographs were taken including a colour standard and scale bar under uniform lighting conditions in a lightbox with a mirrorless digital camera (Olympus). The sex of each animal was determined based on gonad dissection and these data were omitted if there was ambiguity in gonad phenotype.

2.2 | Linear quantification of body shape variation

We quantified various measures of body shape in 10 individuals of each parental species, 491 *Metriaclima* × *Aulonocara* hybrids and 447 *Labidochromis* × *Labeotropheus* hybrids. From photographs, we calculated a series of linear distances (Figure 1b) using ImageJ software (version 2.1.0), including standard length (snout to posterior end of caudal peduncle), head length (snout to opercle), body depth (anterior insertion of dorsal fin to insertion of pelvic fin), caudal peduncle depth, distance between caudal peduncle and anal fin insertion, length of the anal fin base, distance between anal fin and pelvic fin and pectoral fin depth. ImageJ lengths in pixels were converted into centimetres using the scale bar included in each picture. Head proportion was calculated by dividing head length by standard length. To remove the effects of allometry on body measures, all measurements were converted into residual data by normalizing to the standard length, using a dataset including both parents and their hybrids within a single cross. Analyses including linear normalization, ANOVAs, Tukey's Honest Significant Difference post hoc tests and Pearson's correlations were conducted in R (version 3.5.2).

2.3 | Geometric quantification of body shape variation

Body shape variation was also quantified using geometric morphometric shape analysis with a common dataset for all four parental species,

Metriaclima × *Aulonocara* hybrids and *Labidochromis* × *Labeotropheus* hybrids. Homologous anatomic landmarks were defined along the body primarily using fin insertion sites as well as head landmarks such as the snout, eye and opercle (Figure 1a). Coordinate positions of all landmarks were collected from photos using the tpsDig2 software package (version 2.31, <http://www.sbmorphometrics.org/>). Landmark coordinates were extracted and uploaded into the R package geomorph (version 3.1.3) (Adams & Otarola-Castillo, 2013), which was used to conduct Procrustes superimposition of landmarks to remove variation due to size, rotation and position of landmarks to leave variation only due to shape. The effects of allometry were removed with size correction and multiple regression of shape on standard length, using a dataset including all parents and all hybrids. Slopes of vectors of divergence were compared among pairs of groups using the *procD.lm* and *pairwise* functions in *geomorph* (version 3.1.3) using standard length as a covariate and 9999 permutations per function to calculate p-values among 95% confidence intervals (Adams & Otarola-Castillo, 2013).

2.4 | ddRAD-sequencing

Genomic DNA was extracted from caudal fin tissue using DNeasy Blood and Tissue kits (Qiagen). Indexed, double-digestion RADseq libraries were produced as previously described (Burford Reiskind et al., 2016) and sequenced on an Illumina HiSeq with 100 bp paired-end reads (North Carolina State University Genomic Sciences

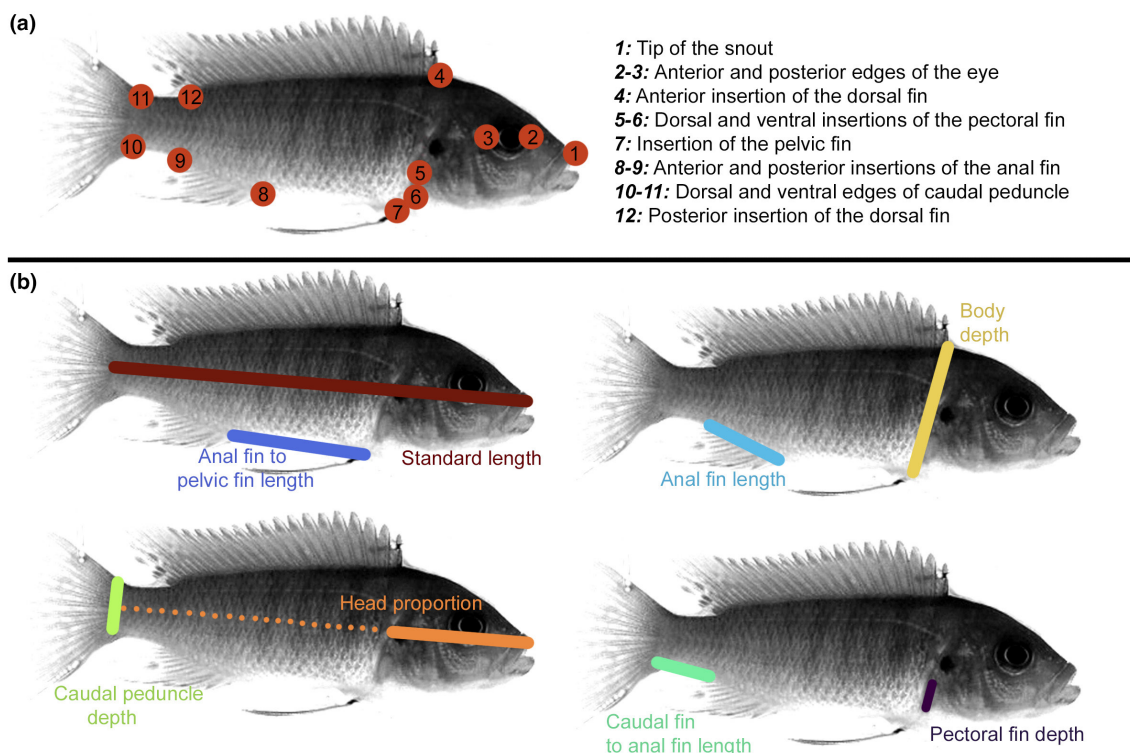


FIGURE 1 Measures used to assess body shape. (a) Geometric and (b) linear measures were used to assess body shape changes commonly seen along benthic-pelagic morphological divergence in fishes. Traits are colour-coded the same throughout the figures.

Laboratory core facility). Raw sequencing data were demultiplexed and low-quality reads were excluded using the program `process_radtags` (Stacks, version 2). The demultiplexed and filtered reads were aligned to the *Maylandia zebra* UMD2a reference genome using BWA with the mem algorithm. We used the programs `pstacks` and `cstacks` (Stacks, version 1) to identify RAD markers in each sample and create a catalogue of RAD markers present in both parents of the cross. The RAD markers of the progeny were subsequently matched against this catalogue with the program `sstacks` (Stacks, version 1). Genotype calls for biallelic markers with alternative alleles between the parents of the cross (aa \times bb markers) were generated with the program `genotypes` (Stacks, version 1), requiring a minimum stack depth of 3 in order to export a locus in a particular individual. As mentioned above, in the *Metriaclima* \times *Aulonocara* cross an inadvertent fertilization event led to two grandsires. To mitigate potential genetic variation introduced by this and focus on species-level differences, markers were only used if both *Aulonocara* sires shared the same homozygous genotype and Hardy-Weinberg equilibrium was met. Any phenotypic effects of genetic variation from a single grandsire (that is intraspecies variation) are expected to be diluted in this cross and therefore not be identified in the subsequent QTL mapping described below.

2.5 | Linkage map

The genetic map was built on the R statistical platform (version 4.0.3) with the package `R/qtl` (version 1.44-9) (Broman, 2009) and in-house scripts available at <https://github.com/kpowder/Biology2022>. RAD markers were sorted and binned in linkage groups according to their position in the *M. zebra* UMD2a reference genome. Markers located in linkage groups with more than 20% of missing data and markers located in unplaced scaffolds with more than 40% of missing data were filtered out from the dataset. A chi-square test was performed with the function `geno.table()` to detect markers with distorted segregation patterns; markers with a Bonferroni-corrected *p*-value <0.01 were removed. The pairwise recombination frequencies among markers were calculated, and an initial map was estimated with the functions `est.rf()` and `est.map()`. Markers in linkage groups that did not show evidence of being misplaced were considered to be inflating the map and removed if they increased the size of the map by at least 6 centiMorgans (cM) and their flanking markers were less than 3 Mb apart. Markers located in unplaced scaffolds were integrated into a given linkage group if they had recombination frequency values <0.15 with at least five markers from that linkage group. The remaining markers located in unplaced scaffolds were removed from the map. Markers whose recombination frequency profile did not match their position in the genetic map, likely due to being located in structural variants or misassembled regions of the reference genome, were rearranged manually in order to minimize the number of crossovers. The function `calc.errorlod()` was used to detect genotyping errors; genotypes with a LOD score ≥ 3 were set as missing data. The map was pruned using a non-overlapping window

algorithm that selected the marker in a given 2 cM window with the least amount of missing data. The final map was estimated and the maximum likelihood estimate of the genotyping error rate (0.0001) was obtained with the function `est.map()`. The final genetic map for *Metriaclima* \times *Aulonocara* hybrids included 22 linkage groups, 1267 total markers, 19–127 markers per linkage group and was 1307.2 cM in total size. The final genetic map for *Labidochromis* \times *Labeotropheus* hybrids included 22 linkage groups, 1180 total markers, 42–81 markers per linkage group and was 1239.5 cM in total size.

2.6 | Quantitative trait loci (QTL) analysis

Quantitative trait loci mapping used multiple-QTL mapping (MQM) methods. Scripts are described in and available from (Powder, 2020), follow (Jansen, 1994) and use the `R/qtl` package (version 1.44–9) (Arends et al., 2010; Broman et al., 2003). The process begins with a liberal scan for unlinked QTL using the `onescan` function in `R/qtl` (Broman, 2009). Putative QTL with a LOD approaching or above 3.0 were used to build a more rigorous statistical model. The MQM method uses these putative loci as cofactors during a QTL scan, verified by backward elimination. The inclusion of cofactors in the final model provides more accurate detection of QTL and assessment of their effects (Jansen, 1994). The statistical significance of QTL was assessed using 1000 permutations. For QTL peaks meeting 5% (significance) or 10% (suggestive) level, 95% confidence intervals were determined using Bayes analysis. Scan details such as cofactors used and significance levels are reported in Table S1.

Markers are named based on contig and nucleotide positions in the *M. zebra* (zebra mbuna) reference genome, *M. zebra*_UMD2a assembly. Names, ID numbers and start/stop positions of candidate genes within QTL intervals were extracted from the NCBI genome data viewer (<https://www.ncbi.nlm.nih.gov/genome/gdv>) gene track for *M. zebra* annotation release 104. If upper and lower limits of the 95% interval were markers that mapped to unplaced scaffolds, the closest marker that mapped to a placed scaffold was used instead. Gene names were compiled from the Database for Visualization and Integrated Discovery (DAVID) (Huang et al., 2009a, 2009b) using NCBI gene ID numbers as a query.

2.7 | Comparisons with other species

Quantitative trait loci intervals from other studies on body shape in different cichlid species (Franchini et al., 2014; Fruciano et al., 2016; Navon et al., 2017), sticklebacks (Albert et al., 2008; Conte et al., 2015; Liu et al., 2014; Rogers et al., 2012; Yang et al., 2016) and carp (Laghari et al., 2014) were compiled, selecting for traits that were comparable with those studied here (i.e. similar measures to Figure 1). Orthologous positions in the *M. zebra* (zebra mbuna) UMD2a genome assembly were identified through manual Basic Local Alignment Search Tool (BLAST, <https://blast.ncbi.nlm.nih.gov/Blast.cgi>) to the *M. zebra* RefSeq genome (UMD2a

assembly). For studies that only provided candidate genes within intervals (Franchini et al., 2014; Yang et al., 2016), cDNA sequences were used a query for a BLAST. For studies that included marker information (Albert et al., 2008; Conte et al., 2015; Laghari et al., 2014; Liu et al., 2014; Navon et al., 2017; Rogers & Jamniczky, 2014), these regions were used as a query for a BLAST. For comparisons within cichlids, the 100 bp surrounding the nucleotide position of the marker position was used. For previous studies in stickleback or carp, the ~400–600 bp sequence of these markers was obtained from the NCBI Nucleotide database and used as a query. The physical positions in the *M. zebra* UMD2a genome were converted to genetic distances using the linkage map assembled for the *Metriaclima* \times *Aulonocara* cross. We cross-referenced these regions and verified synteny using pairwise comparisons on the online tool Genomicus (<https://www.genomicus.bio.ens.psl.eu>) (Nguyen et al., 2022). Any regions with unclear orthologs or synteny were removed. Additional details such as traits and source of QTL information from previous studies are included in Table S7.

3 | RESULTS

3.1 | Body shape variation

Body shape in the four parental species differs in measures such as body depth and relative head proportions, which are common changes across benthic-pelagic divergence in fishes, though differences were not observed in all measures taken (Figures S1, S2 and Table S2). For both crosses, F_2 hybrids are largely intermediate in phenotype to the two parental species, though phenotypic variation in hybrids is increased and can surpass the morphological range of parental species (Figures 2, S1, S2). Lake Malawi cichlids are best characterized as a 'hybrid swarm', in which a set of standing ancestral polymorphisms are being shuffled in differing combinations among species (Brawand et al., 2014; Malinsky et al., 2018; Svardal et al., 2020). Thus, even for shapes with non-significant differences between parental species, QTL mapping can identify genetic loci that underlie shape variation within this clade and genetic combinations that are possible in other species (e.g. see pectoral fin depth for both crosses in Figures 3, 4, S1, S2).

Geometric morphometric shape analysis identifies coordinated changes in body shape in the bodies of the four parental species and F_2 hybrids from both crosses (Figures 2, S3). Together, the first three principal components describe 64.2% of total shape variation (TSV) (Figure S3). Principal component 1 (PC1, 45.0% TSV) describes coordinated changes in body depth, eye size, placement of the pectoral and pelvic fins and head proportions (Figure S3); these are all phenotypes associated with benthic-pelagic divergence across fishes (Cooper et al., 2010; Elmer et al., 2010; Gow et al., 2008; Hulsey et al., 2013, 2018; Schlüter & McPhail, 1992). Notably, the four parental species are distinguished along this primary morphological axis (Figure 2), with *Aulonocara* representing a negative PC1

score, *Metriaclima* and *Labidochromis* occupying the middle of the PC1 axis, and the *Labeotropheus* species having positive PC1 scores (Figure 2). The parents used in each cross demonstrate significantly different shapes (*p*-values for pairwise comparisons of *Aulonocara* vs. *Metriaclima* = $4e^{-7}$, *Metriaclima* vs. *Labidochromis* = 0.9999 and *Labidochromis* vs. *Labeotropheus* $< 1e^{-7}$) (Figure 2). In other words, the two crosses used represent a divergence in opposite directions along a common continuum of body shape. In all, PC1 segregates parental species (Figure 2b) and encompasses a large amount of total body shape variation (45%). Combined with the fact that parental variation is dominantly parallel to this axis (Figure 2a), these indicate the ecological relevance of this single principal component axis of shape.

Given that PC1 is biologically and ecologically informative, we focus just on this shape axis for the rest of the manuscript. This approach reduces a multivariate analysis of body shape to a single variate (i.e. just 45% of total shape variation). Therefore, we compared the angle of shape vectors among parental pairs to compare if the direction of multivariate shape (i.e. analysis including all principal components and 100% of total shape variation) was similar in the two crosses. No pair of parental species was significantly different in the vector angle of divergence ($p=0.2383$ – 0.9130 , Table S3), suggesting that the direction of their shape divergence is largely parallel and therefore predominantly represented by PC1 score. However, we do note that the *Metriaclima* \times *Aulonocara* F_2 hybrids and *Labidochromis* \times *Labeotropheus* F_2 hybrids did diverge in the direction of shape variation from each other ($p=0.001$), though largely not from any of the parental populations (Table S3). One possible reason why these hybrid populations may diverge in multivariate shape, while the parental species do not, is the degree of transgressive phenotypes in the *Metriaclima* \times *Aulonocara* F_2 hybrids. In contrast, the phenotypes of the *Labidochromis* \times *Labeotropheus* F_2 hybrids largely fell within the phenotypic range of their parental species (compare range of hybrid phenotypes in Figure 2a, or range of hybrid phenotypes compared to parents in Figures S1b–d vs. S2b–d). We also observed that PC2 (11.6% TSV and describing relative body depth without changes in head proportion, Figure S3) significantly distinguishes the *Metriaclima* \times *Aulonocara* cross parents (Figure S1), but not the *Labidochromis* \times *Labeotropheus* parents. Alternatively, PC3 (7.6% TSV representing head proportion and fin positioning, Figure S3) is distinct between the *Labidochromis* and *Labeotropheus* parents (Figure S2) but not between *Aulonocara* and *Metriaclima* parents. The fact that these additional shape axes diverge between the crosses suggests that the primary divergence represented by PC1 is then fine-tuned towards specific ecological and functional optima.

Compared to *Metriaclima*, *Aulonocara* have significantly longer head proportions and a commensurate decrease in mid-body length as measured by the length between the anal and pelvic fins (Figure S1 and Table S2). In agreement with linear measurements, *Aulonocara* fishes are significantly associated with a negative PC1 score (Figures 2, S1 and Table S2), which characterizes a body with a larger head, a larger eye and posterior shifts of the dorsal, pelvic and pectoral fins (Figures S1, S3 and Table S2).

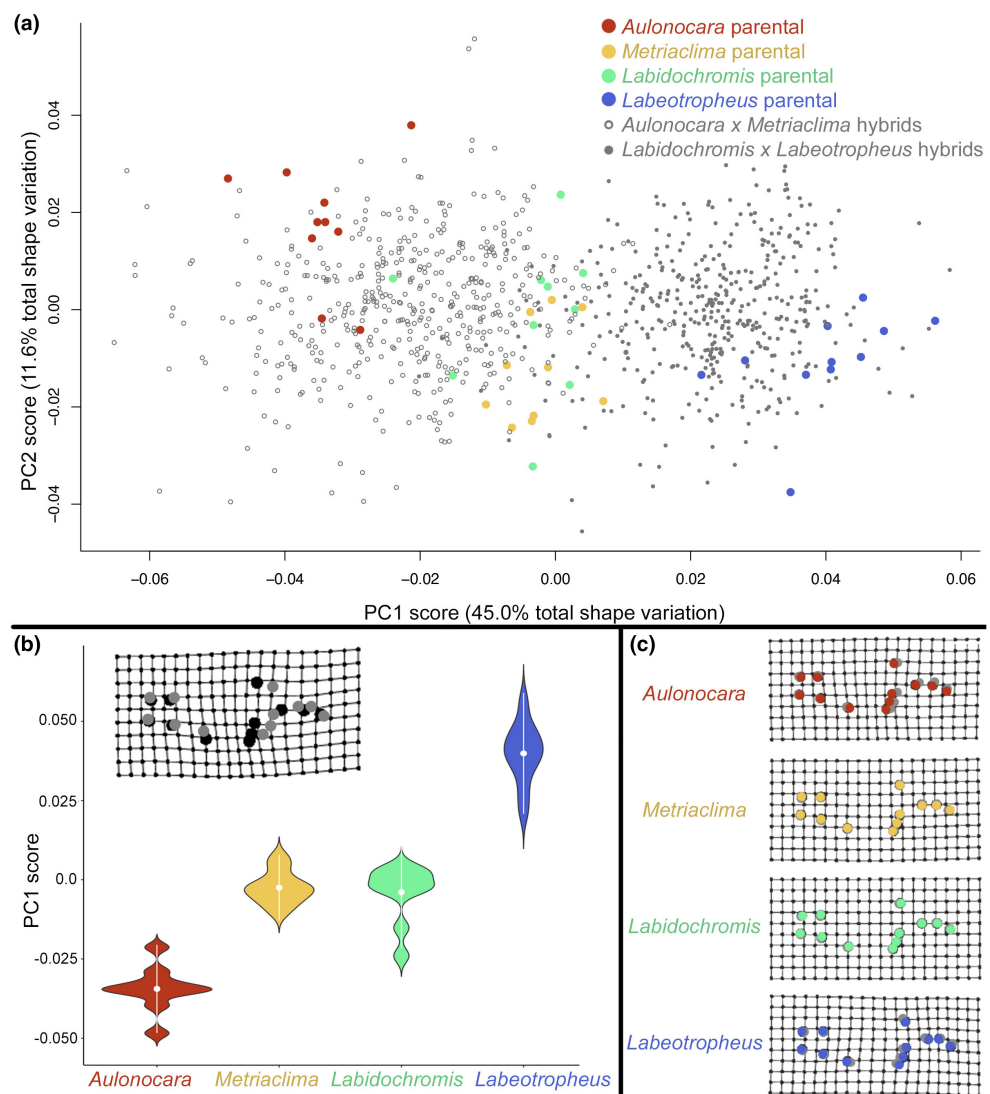


FIGURE 2 Parental species represent distinct body shapes along a primary ecomorphological axis of Lake Malawi cichlids. (a) Overall body shape variation including both crosses, represented by principal component (PC) scores calculated from geometric morphometric measures. Shapes indicated by PC scores are illustrated in Figure S3. (b) As visualized by Principal component 1 (PC1) scores, the *Metriaclima* × *Aulonocara* cross and *Labidochromis* × *Labeotropheus* cross largely represent distinct phenotypes along the primary axis of body shape variation. Inset compares shape at the extremes of the PC1 axis, with negative and positive shape represented by black and grey dots, respectively. This axis describes variation in body depth, head proportion, eye size and relative fin placement, paralleling benthic-pelagic divergence in fishes. All pairwise comparisons of parental groups are statistically significant ($p < 1.4e^{-6}$) except *Metriaclima* sp. and *Labidochromis* sp., which are not significantly different in PC1 scores. (c) Mean body shapes for each parental species, with parental phenotypes represented by coloured dots (locations as in Figure 1a) compared to the consensus shape in grey dots.

Despite both being rock-dwelling Lake Malawi cichlids that live in sympatry (Konings, 2016), *Labidochromis* and *Labeotropheus* parents have more significant phenotypic differences than the *Aulonocara* and *Metriaclima* species pair (Figures 2, S1, S2 and Table S2). *Labeotropheus* species are specialized benthic fishes within Lake Malawi (Cooper et al., 2010), and have significantly shorter head regions, decreased body depth, decreased caudal peduncle depth, decreased anal fin length and increased length between the caudal peduncle and the anal fin compared to *Labidochromis* fish (Figure S2 and Table S2). In agreement with these linear measures, *Labeotropheus* is significantly associated

with a positive PC1 score, associated with a narrower body shape, shorter head proportion and shorter anal fin (Figures S2, S3 and Table S2).

3.2 | Sexual dimorphism in body shape

Differences between males and females, termed sexual dimorphism, are incredibly common across species and often include differences in body size or shape (Badyaev, 2002; Fairbairn et al., 2007; Frayer & Wolpoff, 1985; Williams & Carroll, 2009). We

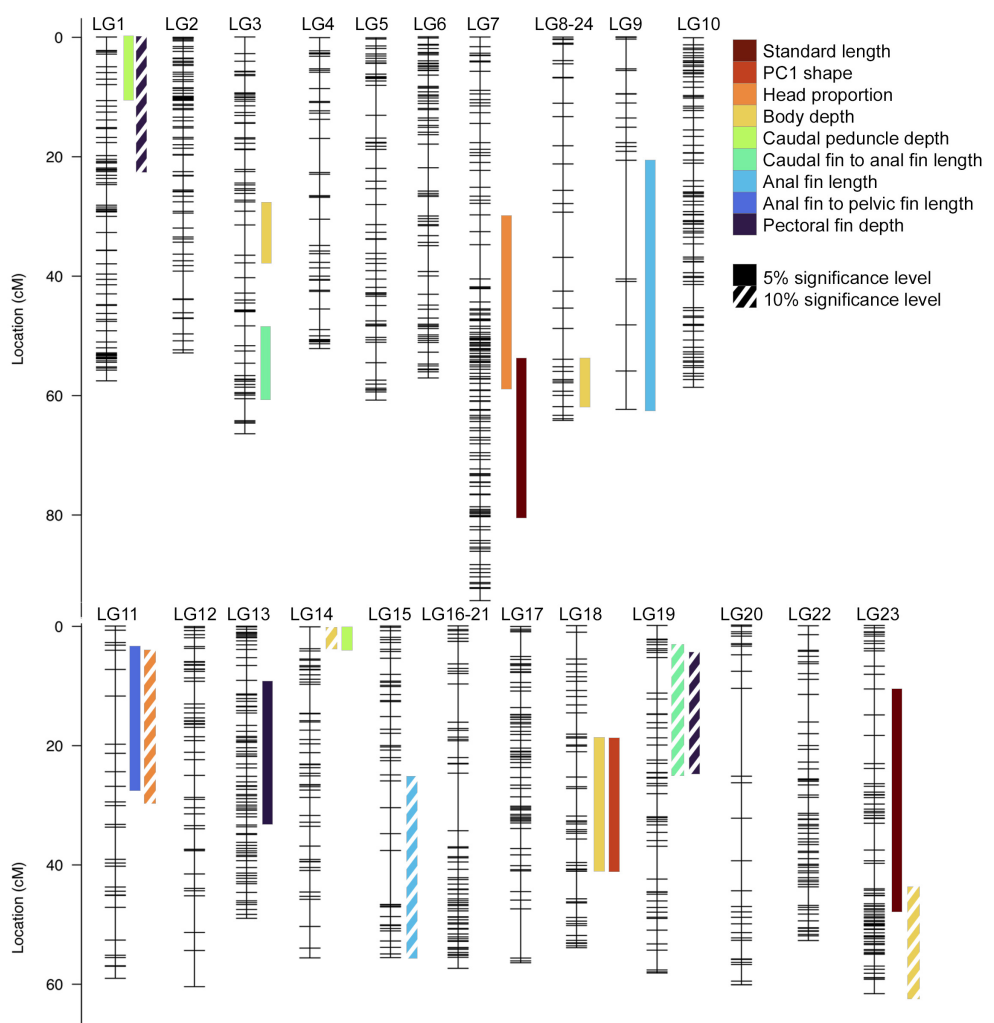


FIGURE 3 Quantitative trait loci (QTL) mapping identifies 20 intervals associated with changes in body shape between *Metriaclima* and *Aulonocara*. Each linkage group (LG, i.e. chromosome) is indicated with genetic marks noted by hash marks. The phenotype related to each QTL region is indicated by colour. Solid bars are significant at the 5% genome-wide level, while those with white diagonals are suggestive, meeting the 10% genome-wide level. Bar widths indicate 95% confidence interval for the QTL, as calculated by Bayes analysis. Illustrations of phenotypes are in Figures 1, S1, S3 and S4. QTL scans at the genome and linkage group level are in Figures S1 and S4, respectively. Details of the QTL scan including markers and physical locations defining each region are in Table S1.

therefore assessed differences between sexes in our two hybrid populations. Sex in Lake Malawi cichlids is genetically determined, with a diversity of sex determination loci identified (Gammerdinger & Kocher, 2018). Within the *Labidochromis* × *Labeotropheus* cross, sex is not associated with common sex determination loci, and of the 354 animals for which sex was called, 92.9% were male. In the *Metriaclima* × *Aulonocara* cross, sex is solely determined by a common XY system on LG7, which produces an even one-to-one sex ratio (Peterson et al., 2017; Ser et al., 2010). Thus, we only discuss sexual dimorphism based on 412 *Metriaclima* × *Aulonocara* hybrids (48.1% male), though see Table S2 for full ANOVA analyses in both crosses.

Overall size was the most significant body shape difference between males and females (standard length, Table S2). Within the linear measures of body shape, males had significantly larger head proportions, body depth and length of the anal fin, which features

egg spot pigmentation patterns used during mating (Table S2). This is supported by dimorphism in geometric morphometric shape analyses, with males being associated with a negative PC1 score, including increased body depth and a larger head proportion (Figure S3 and Table S2).

3.3 | Genetic basis of body shape variation

To determine the genetic mechanisms that underlie variation in body shape, we genetically mapped PC1 score representing complex shape changes (Figures 2, S3) and eight linear measures (Figure 1) to not only identify the genetic origins of each trait, but also compare these across different aspects of body shape. By doing this in both the *Metriaclima* × *Aulonocara* cross and *Labidochromis* × *Labeotropheus* cross that represent distinct body shapes within Lake Malawi

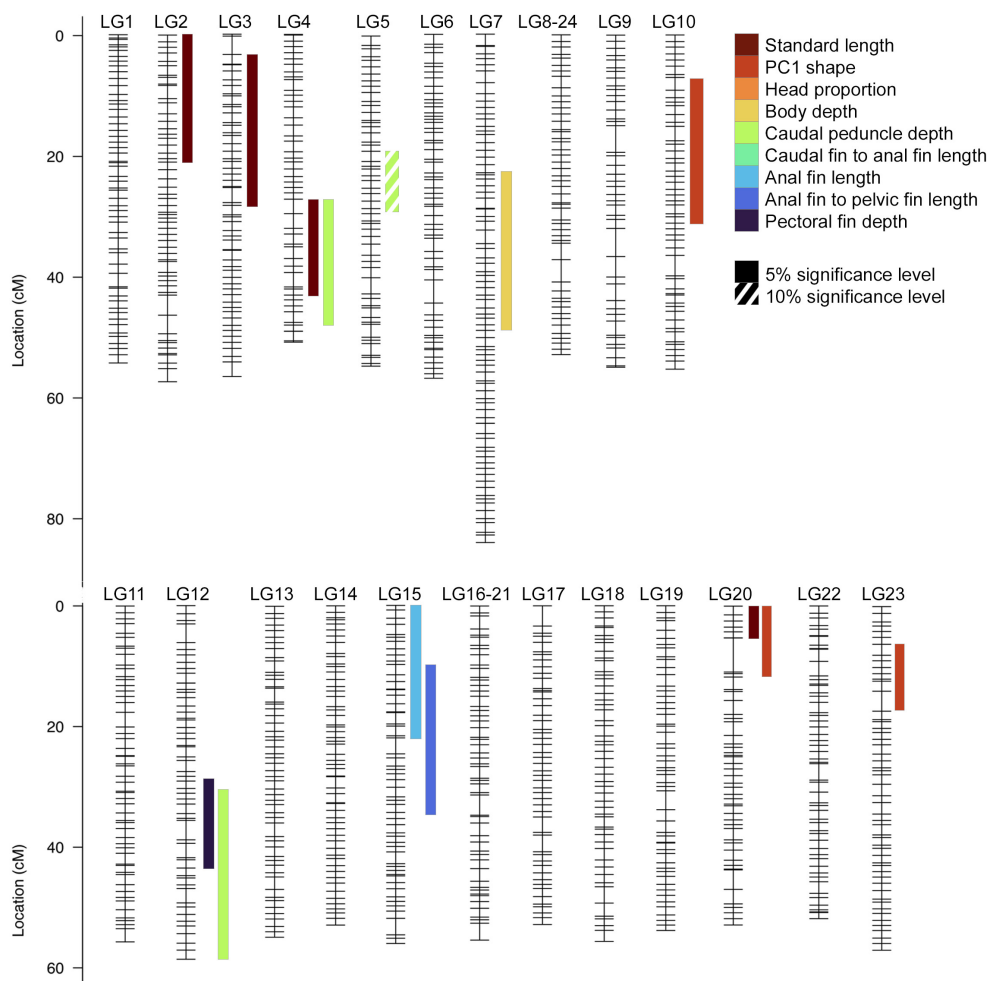


FIGURE 4 Quantitative trait loci (QTL) mapping identifies 14 intervals associated with changes in body shape between *Labidochromis* and *Labeotropheus*. Data are as presented in Figure 3. Illustrations of phenotypes are in Figures 1, S2, S3, and S5. QTL scans at the genome and linkage group level are in Figures S2 and S5, respectively. Details of the QTL scan including markers and physical locations defining each region are in Table S1.

cichlids, we could also evaluate if common mechanisms control the evolution of body shape in distinct directions along a continuum of morphological variation (Figure 2).

Twenty genetic intervals underlie the quantitative differences in body shape in *Metriaclima* × *Aulonocara* F₂ hybrids. This includes 13 that reach 5% statistical significance at the genome-wide level and 7 that are suggestive, reaching 10% significance levels (Figures 3, S1, S4 and Table S1). Each trait has 1–5 genetic intervals that influence phenotypic variation. QTL intervals are spread throughout the genome, with 12 of 22 linkage groups each containing 1–2 loci. QTL regions explain from 3.2% to 7.6% of the total variation in each trait (Table S1 and Figure S4), meaning that all body shapes analysed are controlled by many genetic loci, each with a small effect.

A total of 13 significant and one suggestive QTL were identified in the *Labidochromis* × *Labeotropheus* F₂ hybrids, with 0–4 QTL per trait (Figures 4, S2, S5 and Table S1). Like the other cross, QTL are spread throughout the genome, with 10 of 22 linkage groups containing 1–2 QTL each. Phenotypic traits are similarly complex in terms of genetics, with each QTL only accounting for 3.4–8.6% of

shape variation (Figure S5). Even for the trait with the most variation explained (body depth in *Metriaclima* × *Aulonocara*), only 19.3% of total shape variation is explained by the combined effects of 5 QTL (Figure S4 and Table S1).

Quantitative trait loci between the two crosses are largely non-overlapping both generally and for specific traits (Figures 3, 4, S1–S5 and Table S1). The linkage groups that contain 'hotspots' with multiple QTL in one cross are largely absent from QTL in the other cross. For example, LGs 1, 11, 14, 18 and 19 each contain two overlapping QTL in the *Metriaclima* × *Aulonocara* cross, however, none of these LGs have a single QTL in the *Labidochromis* × *Labeotropheus* cross. Alternately, LGs 4, 12 and 20 each contain two overlapping QTL in *Labidochromis* × *Labeotropheus* cross, but no QTL in the *Metriaclima* × *Aulonocara* cross. This lack of common genetic signals is also the case when looking at individual traits. There is only one instance where the same trait maps to the same LG. In both crosses, LG15 contains a QTL for anal fin length (Figures 3 and 4). However, the 95% confidence intervals do not overlap, residing 23 Mb away from each other (Figures 3, 4 and Table S1). Thus, two distinct

genetic intervals control anal fin length in these crosses, but both happen to occur on the same linkage group.

However, there are some overlapping QTL within each cross, indicating that certain genomic intervals may have pleiotropic effects on body shape (Figures 3, 4 and Table S1). First, two QTL from the *Metriaclima* × *Aulonocara* cross overlap from 56.3 to 58.0 cM on LG7, contributing to variation in standard length and head proportion (Figure 3). Notably, both traits are sexually dimorphic (Table S2), and the Y sex-determining locus is nearby at 61.4–62.9 cM (Peterson et al., 2017). Second, QTL for head proportion and the distance between the anal and pelvic fins overlap on LG11 in the *Metriaclima* × *Aulonocara* cross, residing at 3.2–29.5 cM. This 'hotspot' may be explained by a large, previously characterized chromosomal inversion on LG11 between *Metriaclima* sp. genomes and *Aulonocara* sp. genomes (Conte et al., 2019). Finally, two QTL co-localize in the *Labidochromis* × *Labeotropheus* cross from 29.2 to 58.8 on LG12. This region underlies phenotypic variation in pectoral fin depth and caudal peduncle depth. This region of LG12 is also notable for a series of structural differences and changes in recombination rates among cichlid species (Conte et al., 2019). Thus, interspecific variation in structural features of the genome may account for instances where QTL for disparate traits map to common intervals.

Allelic effects on phenotypes have a distinct trend for PC1 score in both crosses (Figures S4, S5 and Table S1). Namely, the allele inherited from the parent associated with a more positive PC1 score (Figure 2) increases this trait value in hybrids (1 QTL for *Metriaclima* × *Aulonocara* and 3 QTL for *Labidochromis* × *Labeotropheus* (Figures S4, S5 and Table S1)). However, other than this trait, there are no clear trends when looking at allelic effects on phenotypes in either cross. For example, standard length in the *Labidochromis* × *Labeotropheus* cross is not significantly different between species, is controlled by 4 QTL, and at all four of these loci the derived *Labeotropheus* allele increases size, through a mixture of additive, overdominant and underdominant inheritance (Figure S5a).

Additional work will be needed to further clarify the molecular mechanisms through which phenotypic variation is generated. While some intervals have relatively few candidate genes (e.g. QTL for body depth on LG14 with only 11 genes), most of our intervals contain hundreds of genes (Tables S5 and S6). While it is too early to speculate on the effects of specific candidate genes in these intervals, we looked for overlap between our body QTL and one gene previously implicated in trophic adaptations that commonly co-occur with body shape variation in cichlids (Cooper et al., 2010). *Ptch1* variation produces alternate shapes in the lower jaw that represent a trade-off between two feeding mechanisms: suction feeding associated with more pelagic species and biting that is common within specialized benthic species (Roberts et al., 2011). *Ptch1* co-localizes with the LG12 QTL hotspot in the *Labidochromis* × *Labeotropheus* associated with depth of both the pectoral and caudal fins. Though this region is also associated with altered patterns of recombination, this leaves open the possibility that a gene such as *ptch1* may have pleiotropic effects on multiple phenotypes associated with cichlid divergence.

3.4 | Modularity of body shape variation

The presence of genetic intervals linked to multiple phenotypes suggests that a single locus may have pleiotropic effects on multiple aspects of body shape variation. We wished to further address whether body shape variation involves coordinated changes, or if different aspects of body shape may be able to evolve independently. To directly address the relationships among our measured phenotypes, we assessed correlations between all pairs of traits. For both crosses, standard length was positively and strongly associated with linear measures (e.g. r values from 0.846 to 0.963 in the *Metriaclima* × *Aulonocara* cross, Table S4). Note that geometric morphometric analysis includes a size correction prior to principal component analysis. After removing the effects of size, residuals for each measure were not strongly correlated with each other (r values from -0.563 to 0.369 with a mean of -0.015 in the *Metriaclima* × *Aulonocara* cross, and r values from -0.412 to 0.340 with a mean of 0.011 in the *Labidochromis* × *Labeotropheus* cross) (Table S4). While additional analysis such as examination of morphological integration will be important to further define these patterns of shape co-variation, this lack of correlation among phenotypes suggests that despite some traits having overlapping genetic influences (i.e. QTL), the phenotypic patterns generated are distinct.

4 | DISCUSSION

4.1 | Evolution of an ecologically important trait

We sought to understand the genetics of an ecologically important trait, body shape, using multiple hybrid crosses of Lake Malawi cichlids and a series of both linear and geometric shape measurements. We find numerous differences in body shape including body depth, head proportions, caudal peduncle depth and shifting of fin insertions that are likely to have functional consequences for swimming manoeuvres. This series of changes in the body plan seen in the cichlids used here mirrors variation commonly seen along the benthic-pelagic axis in fishes. Further, the divergence of body shape between sympatric *Labidochromis* and *Labeotropheus* emphasizes that while these fish encounter similar functional challenges of living in a complex rocky habitat, their distinct trophic niches are key factors driving variation in body shape. Specifically, the insectivore *Labidochromis* has larger head proportions, increased body depth, a deeper caudal peduncle, a shorter caudal region and a longer anal fin than the algae-scraping *Labeotropheus* (Figure S2, Table S2) (Konings, 2016). These adaptations in *Labidochromis* are similar to fishes that use quick bursts of speed with abrupt shifts in direction (Meyers & Belk, 2014; Webb, 1984), and may reflect an ability of *Labidochromis* to quickly manoeuvre and pursue insect prey, while *Labeotropheus* feed by hovering and holding steady within water flows of the lake to graze on algae.

We then used QTL mapping to identify the genetic basis of these differences in body shape. We predicted that the same genetic

intervals would influence body shape traits in both crosses, given that these crosses represent different aspects of the same continuum of shape variation (Figure 2). In other words, producing an elongated body shape would be the same regardless of relative starting body shape. Contrary to our prediction, we found that QTL that control body shape variation between the open water *Aulonocara* and benthic *Metriaclima* fishes are distinct from those that influence variation between a benthic insectivore like *Labidochromis* and the benthic specialist *Labeotropheus* (Figures 3, 4 and Table S1). This trend occurred for both a series of linear measures of body shape as well as for a measure of coordinated changes in body shape (Figure 1). It is possible that the identification of QTL was limited by our analytical approach. Specifically, PC1 score represented a large degree of total variation in body shape among the nearly 1000 animals measured (Figure 2) and parental species did not vary in their direction of shape variation in a multivariate analysis of body shape (Table S3). Nonetheless, we may not have identified overlapping QTL for body shape (Figures 3 and 4) as we limited our genetic mapping to univariate measures of shape (i.e. PC1 score or linear measures) and the two hybrid populations did significantly vary in the direction of shape variation when accounting for multivariate measures of shape (Table S3). Despite these limitations, the lack of overlapping QTL coupled with the modest effects of each QTL (3.2–8.6% variation explained per loci, Table S1 and Figures S4, S5) emphasize that body shape is a complex, polygenic trait and similar morphologies can be produced by multiple mechanisms (a many-to-one relationship).

4.2 | Distinct genetic signals regulate body shape across fishes

Body elongation in fishes along the benthic-pelagic axis occurs repeatedly and widely across fish phylogeny, independent of time (modern vs. historic) and environment (marine vs. freshwater) (Burns & Sidlauskas, 2018; Friedman et al., 2020; Gow et al., 2008; Hulsey et al., 2013; Muschick et al., 2012; Ribeiro et al., 2018; Robinson & Wilson, 1994). In 'replaying life's tape' (Gould, 1989), it is clear that fishes have converged on similar body shapes based on ecological selection. However, it remains unknown if fish species use similar genetic mechanisms to achieve these predictable morphologies. Towards this goal, we compared the QTL in this study with QTL identified in additional Lake Malawi species (Navon et al., 2017), crater cichlids from Central America (Franchini et al., 2014), parallel radiations of sticklebacks (Albert et al., 2008; Conte et al., 2015; Rogers et al., 2012; Yang et al., 2016) and carp (Laghari et al., 2014) (Figure 5, Table S7). This comes with caveats such as missing data due to unclear orthologous regions in the *M. zebra* genome used here, the inclusion of only some fish species, and similar, yet not identical measures in other studies. Despite this, our comparative approach can still identify if these parallel divergences in body shape could share common genetic mechanisms across multiple fish clades.

Overall, we find relatively minimal overlaps in QTL from our study and previous analysis of body shape in other fishes (Figures 3–5). For instance, regions that have multiple QTL in this work (e.g. LGs 1 and 19 for the *Metriaclima* × *Aulonocara* cross or LGs 4 and 20 for the *Labidochromis* × *Labeotropheus* cross) have not been identified in previous analyses. However, there are two instances where there is an overlap in QTL from this study and previous studies, which also describe similar traits. The first is on LG7, where a QTL for head proportion in *Metriaclima* × *Aulonocara* overlaps with a QTL for head length in carp (Laghari et al., 2014) from 52.27 to 58.01 cM (Figures 3 and 5). A second overlap occurs on LG10, which has been associated with QTL in three of the previous seven studies (Figure 5). One of these overlaps with a QTL from this study, for PC1 shape in the *Labidochromis* × *Labeotropheus* cross. Interestingly, 9.16–13.41 cM on LG10 is associated with body depth in other Lake Malawi cichlids (Navon et al., 2017), and PC1 shape in our work also describes differences in relative body depth (Figures 2, S3). While this small number of overlapping intervals may identify common genetic intervals that regulate body shape in multiple species, we largely find that the evolution of similar body shapes is due to divergent genetic mechanisms, both within cichlids and across fishes.

4.3 | Impacts of evolutionary history on genetic architecture and modularity

Most body shape variation in stickleback fish is caused by few genes with large effects (10–20% variation explained each) and clustered 'supergene' regions that influence multiple phenotypes associated with benthic ecologies (Albert et al., 2008; Liu et al., 2014; Miller et al., 2014; Yang et al., 2016). In contrast to this, we find that body shape variation in Lake Malawi cichlids is due to many genes, each with a small effect (Figures S4, S5 and Tables S1, S5 and S6). Additionally, we find that QTL are largely spread throughout the genome (Figures 3 and 4), and there are minimal correlations between measurements (Table S4). The largely modular basis of body shape variation in cichlids has implications for evolutionary potential (i.e. evolvability) and phenotypic variation (Melo et al., 2016; Pigliucci & Muller, 2010; Wagner et al., 2007). Namely, as distinct phenotypes are largely controlled by discrete genetic intervals in cichlids, this allows independent evolution of distinct morphologies, each of which could be subject to different patterns of selection.

While most of the genetic correlations identified show independent segregation and phenotypic impacts, there are exceptions. One is found at the sex determination locus on LG7 in the *Metriaclima* × *Aulonocara* cross, where the multiple traits mapped to this region are also sexually dimorphic. Our study is unable to disentangle whether the LG7-associated trait variation is sex limited (i.e. modulated by sex-specific physiology during development, where sex is correlated to LG7 genotype), or results from allelic variation that is in linkage with the sex determination locus. If future

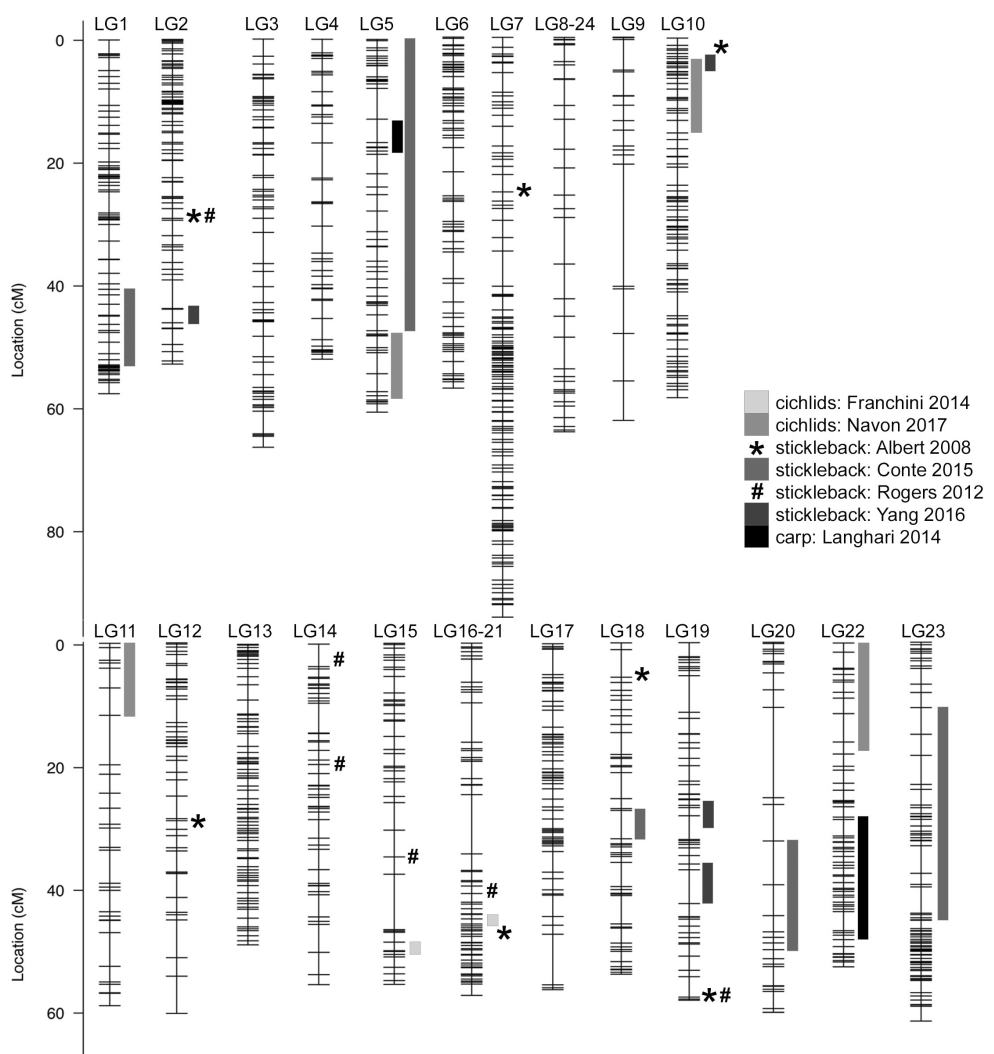


FIGURE 5 Comparison with QTL intervals previously identified in other cichlids, stickleback and carp reveals little overlap with QTL determined in this study. Reported QTL from the indicated reference were converted to physical locations in the *M. zebra* genome UMD2a assembly and mapped onto the *Metriaclima* × *Aulonocara* genetic map. Bar widths indicate the 95% confidence interval for the QTL as calculated by each study. Those studies that reported QTL peak positions, but not confidence intervals, are indicated by * and # symbols. Details of phenotypes associated with each interval, physical locations and methods of converting to UMD2a genome positions are detailed in Table S7.

studies indicate the latter, this would support the hypothesis that sexual dimorphism in body morphology evolves from an accumulation of sexually antagonistic alleles at sex determination loci, as has been suggested for sexual dimorphism in pigmentation (Albertson et al., 2014; Roberts et al., 2009). Two other hotspots containing multiple trait QTL include LG11 in the *Metriaclima* × *Aulonocara* cross and LG12 in the *Labidochromis* × *Labeotropheus* cross. There is clear evidence for an interspecific inversion at LG11 between *Metriaclima* and *Aulonocara*, and recombination patterns among different hybrid crosses suggest that LG12 has significant variation in structure among Lake Malawi cichlids (Conte et al., 2019). Inversions and other structural variants can strongly suppress recombination, and this could support the evolutionary accumulation of complementary adaptive alleles at multiple loci within broad haplotypes. Similar roles for inversions have been suggested in the parallel adaptation of

sticklebacks (Jones et al., 2012), including the predictable fixation of certain inversion haplotypes within freshwater populations (Roesti et al., 2015). Within the Lake Malawi radiation, where occasional interspecific hybridization occurs and likely supports evolution, inversions may preserve combinations of alleles that drive multiple, distinct traits in the same direction along body shape ecomorphological axis, while avoiding discordant phenotypes. Our observations indicate a need for additional work dissecting genetic variation at structural variants. This could determine whether multiple genes are involved, or whether the hotspots represent the pleiotropic effects of a single gene that happens to lie within a structural variant.

This different genetic architecture and pattern of genetic modularity within stickleback and cichlid fishes is likely due to their different evolutionary histories and ancestral states. Specifically, ancestral sticklebacks are marine, pelagic morphs

that have a strong selective pressure towards a freshwater, benthic form when migrating into small lakes created by glacial retreat (Schluter & McPhail, 1992; Walker, 1997). On the other hand, cichlids evolved from a small group of generalist, riverine species (Malinsky et al., 2018) in sympatry towards multiple adaptive peaks. While ecological divergence is an important stage of the cichlid radiation and influences patterns of speciation, this is only one of many selective pressures (Kocher, 2004; Streelman & Danley, 2003). Further, the cichlid 'hybrid swarm' has extensive shared genetic variation and ongoing gene flow among fish with varying body shapes, which further influences the genetic architecture, modularity and evolutionary potential of morphological variation in cichlids (Brawand et al., 2014; Malinsky et al., 2018; Svardal et al., 2020).

5 | CONCLUSIONS

Body elongation is common across animals. In fishes, the benthic-pelagic ecomorphological axis is a major source of phenotypic variation, encompassing a suite of body shape phenotypes. Using cichlid species with body shape variation that parallels the benthic-pelagic axis in other fishes, we show that body shape variation is most likely due to distinct molecular signals in different fish clades or even at different points along a morphological continuum in a single radiation. Through comparison of genetic mapping in two hybrid crosses, we show here that even the closely related cichlid species examined have distinct genetic architectures for this convergent trait. The genetic loci we identify here additionally serve as candidates to understand the molecular origins of an ecologically relevant trait, body shape variation.

AUTHOR CONTRIBUTIONS

K.E.P. and R.B.R. designed the research. A.C.B., E.C.M., P.J.C. and N.B.R. performed animal husbandry, photography and collections. N.B.R. prepared sequencing libraries. K.E.P., D.M. and M.J. performed phenotypic measurements. K.E.P., L.D., E.C.M., A.C.B. and R.B.R. analysed data. K.E.P., L.D. and A.A.B. wrote the paper with edits from all authors.

ACKNOWLEDGEMENTS

We thank Dr. Samantha Price, Craig Albertson, Andy Conith and Michelle Gilbert for useful discussion and Dr. Daniela Almeida for useful comments on initial manuscripts. This work was supported by NSF CAREER #1942178 (KEP), NIH P20GM121342 (KEP), NIH R15DE029945 (KEP), NSF IOS-1456765 (RBR) and an Arnold and Mabel Beckman Institute Young Investigator Award (RBR).

DATA AVAILABILITY STATEMENT

Raw sequence data are available at <https://www.ncbi.nlm.nih.gov/bioproject/PRJNA955776>. Additional data are available at Dryad <https://doi.org/10.5061/dryad.4mw6m90cz>. Dryad files

include phenotypic measures, TPS files for geometric morphometric analysis and genotypes used for quantitative trait loci mapping.

ORCID

Leah DeLorenzo  <https://orcid.org/0000-0002-0789-8875>
 Aldo Carmona Baez  <https://orcid.org/0000-0003-0023-3763>
 Emily C. Moore  <https://orcid.org/0000-0001-6166-3367>
 Reade B. Roberts  <https://orcid.org/0000-0003-2551-3761>
 Kara E. Powder  <https://orcid.org/0000-0001-7415-4262>

REFERENCES

Adams, D., & Otarola-Castillo, E. (2013). Geomorph: An r package for the collection and analysis of geometric morphometric shape data. *Methods in Ecology and Evolution*, 4(4), 393–399.

Albert, A. Y., Sawaya, S., Vines, T. H., Knecht, A. K., Miller, C. T., Summers, B. R., Balabhadra, S., Kingsley, D. M., & Schluter, D. (2008). The genetics of adaptive shape shift in stickleback: Pleiotropy and effect size. *Evolution*, 62(1), 76–85. <https://doi.org/10.1111/j.1558-5646.2007.00259.x>

Albertson, R. C., Powder, K. E., Hu, Y., Coyle, K. P., Roberts, R. B., & Parsons, K. J. (2014). Genetic basis of continuous variation in the levels and modular inheritance of pigmentation in cichlid fishes. *Molecular Ecology*, 23(21), 5135–5150. <https://doi.org/10.1111/mec.12900>

Arends, D., Prins, P., Jansen, R. C., & Broman, K. W. (2010). R/QTL: High-throughput multiple QTL mapping. *Bioinformatics*, 26(23), 2990–2992. <https://doi.org/10.1093/bioinformatics/btq565>

Arnold, S. (1983). Morphology, performance and fitness. *American Zoologist*, 23, 347–361.

Arnold, S. (1992). Constraints on phenotypic evolution. *The American Naturalist*, 140, S85–S107.

Badyaev, A. V. (2002). Growing apart: An ontogenetic perspective on the evolution of sexual size dimorphism. *Trends in Ecology & Evolution*, 17(8), 369–378.

Bergmann, P. J., & Irschick, D. J. (2012). Vertebral evolution and the diversification of squamate reptiles. *Evolution*, 66(4), 1044–1058. <https://doi.org/10.1111/j.1558-5646.2011.01491.x>

Brachmann, M. K., Parsons, K., Skulason, S., & Ferguson, M. M. (2021). The interaction of resource use and gene flow on the phenotypic divergence of benthic and pelagic morphs of Icelandic Arctic charr (*Salvelinus alpinus*). *Ecology and Evolution*, 11, 7315–7334.

Brawand, D., Wagner, C. E., Li, Y. I., Malinsky, M., Keller, I., Fan, S., Simakov, O., Ng, A. Y., Lim, Z. W., Bezaury, E., Turner-Maier, J., Johnson, J., Alcazar, R., Noh, H. J., Russell, P., Aken, B., Alfoldi, J., Amemiya, C., Azzouzi, N., ... di Palma, F. (2014). The genomic substrate for adaptive radiation in African cichlid fish. *Nature*, 513(7518), 375–381. <https://doi.org/10.1038/nature13726>

Broman, K. W. (2009). *A guide to QTL mapping with R/qtl*. Springer.

Broman, K. W., Wu, H., Sen, S., & Churchill, G. A. (2003). R/QTL: QTL mapping in experimental crosses. *Bioinformatics*, 19(7), 889–890. <https://doi.org/10.1093/bioinformatics/btg112>

Burford Reiskind, M. O., Coyle, K., Daniels, H. V., Labadie, P., Reiskind, M. H., Roberts, N. B., Roberts, R. B., Schaff, J., & Vargo, E. L. (2016). Development of a universal double-digest RAD sequencing approach for a group of non-model, ecologically and economically important insect and fish taxa. *Molecular Ecology Resources*, 16, 1303–1314. <https://doi.org/10.1111/1755-0998.12527>

Burns, M. D., & Sidlauskas, B. L. (2018). Ancient and contingent body shape diversification in a hyperdiverse continental fish radiation. *Evolution*, 73(3), 569–587.

Claverie, T., & Wainwright, P. C. (2014). A morphospace for reef fishes: Elongation is the dominant axis of body shape evolution. *PLoS One*, 9(11), e112732. <https://doi.org/10.1371/journal.pone.0112732>

Conte, G. L., Arnegard, M. E., Best, J., Chan, Y. F., Jones, F. C., Kingsley, D. M., Schluter, D., & Peichel, C. L. (2015). Extent of QTL reuse during repeated phenotypic divergence of sympatric Threespine stickleback. *Genetics*, 201(3), 1189–1200. <https://doi.org/10.1534/genetics.115.182550>

Conte, M. A., Joshi, R., Moore, E. C., Nandamuri, S. P., Gammerdinger, W. J., Roberts, R. B., Carleton, K. L., Lien, S., & Kocher, T. D. (2019). Chromosome-scale assemblies reveal the structural evolution of African cichlid genomes. *Gigascience*, 8(4), giz030. <https://doi.org/10.1093/gigascience/giz030>

Cooper, W. J., Parsons, K., McIntyre, A., Kern, B., McGee-Moore, A., & Albertson, R. C. (2010). Benthic-pelagic divergence of cichlid feeding architecture was prodigious and consistent during multiple adaptive radiations within African rift-lakes. *PLoS One*, 5(3), e9551. <https://doi.org/10.1371/journal.pone.0009551>

Coyne, J., & Orr, H. (2004). *Speciation*. Sinauer Associates.

Elmer, K. R., Kusche, H., Lehtonen, T. K., & Meyer, A. (2010). Local variation and parallel evolution: Morphological and genetic diversity across a species complex of neotropical crater lake cichlid fishes. *Philosophical Transactions of the Royal Society of London. Series B, Biological Sciences*, 365(1547), 1763–1782. <https://doi.org/10.1098/rstb.2009.0271>

Fairbairn, D., Blackenhorn, W., & Szekely, T. (2007). Sex, size and gender roles. *Evolutionary studies of sexual size dimorphism*. Oxford University Press.

Franchini, P., Fruciano, C., Spreitzer, M. L., Jones, J. C., Elmer, K. R., Henning, F., & Meyer, A. (2014). Genomic architecture of ecologically divergent body shape in a pair of sympatric crater lake cichlid fishes. *Molecular Ecology*, 23(7), 1828–1845. <https://doi.org/10.1111/mec.12590>

Frayer, D. W., & Wolpoff, M. H. (1985). Sexual dimorphism. *Annual Review of Anthropology*, 14, 429–473.

Friedman, S. T., Price, S. A., Corn, K. A., Larouche, O., Martinez, C. M., & Wainwright, P. C. (2020). Body shape diversification along the benthic-pelagic axis in marine fishes. *Proceedings of the Biological Sciences*, 287(1931), 202001053. <https://doi.org/10.1098/rspb.2020.1053>

Friedman, S. T., Price, S. A., & Wainwright, P. C. (2021). The effect of locomotion mode on body shape evolution in teleost fishes. *Integrative Organismal Biology*, 3(1), obab016.

Fruciano, C., Franchini, P., Kovacova, V., Elmer, K. R., Henning, F., & Meyer, A. (2016). Genetic linkage of distinct adaptive traits in sympatrically speciating crater lake cichlid fish. *Nature Communications*, 7, 12736. <https://doi.org/10.1038/ncomms12736>

Gammerdinger, W. J., & Kocher, T. D. (2018). Unusual diversity of sex chromosomes in African cichlid fishes. *Genes (Basel)*, 9(10), 480. <https://doi.org/10.3390/genes9100480>

Gould, S. J. (1989). *Wonderful life: The Burgess shale and the nature of history*. W. W. Norton & Company.

Gow, J., Rogers, S., Jackson, M., & Schluter, D. (2008). Ecological predictions lead to the discovery of a benthic-limnetic sympatric species pair of threespine stickleback in little quarry Lake, British Columbia. *Canadian Journal of Zoology*, 86, 564–571. <https://doi.org/10.1139/Z08-032>

Hatfield, T., & Schluter, D. (1999). Ecological speciation in sticklebacks: Environment-dependent hybrid fitness. *Evolution*, 53(3), 866–873. <https://doi.org/10.1111/j.1558-5646.1999.tb05380.x>

Huang, D. W., Sherman, B. T., & Lempicki, R. A. (2009a). Bioinformatics enrichment tools: Paths toward the comprehensive functional analysis of large gene lists. *Nucleic Acids Research*, 37(1), 1–13. <https://doi.org/10.1093/nar/gkn923>

Huang, D. W., Sherman, B. T., & Lempicki, R. A. (2009b). Systematic and integrative analysis of large gene lists using DAVID bioinformatics resources. *Nature Protocols*, 4(1), 44–57. <https://doi.org/10.1038/nprot.2008.211>

Hulsey, C. D., Holzman, R., & Meyer, A. (2018). Dissecting a potential spandrel of adaptive radiation: Body depth and pectoral fin ecomorphology coevolve in Lake Malawi cichlid fishes. *Ecology and Evolution*, 8(23), 11945–11953. <https://doi.org/10.1002/ece3.4651>

Hulsey, C. D., Roberts, R. J., Loh, Y. H., Rupp, M. F., & Streelman, J. T. (2013). Lake Malawi cichlid evolution along a benthic/limnetic axis. *Ecology and Evolution*, 3(7), 2262–2272. <https://doi.org/10.1002/ece3.633>

Jansen, R. C. (1994). Controlling the type I and type II errors in mapping quantitative trait loci. *Genetics*, 138(3), 871–881.

Jones, F. C., Grabherr, M. G., Chan, Y. F., Russell, P., Mauceli, E., Johnson, J., Swofford, R., Pirun, M., Zody, M. C., White, S., Birney, E., Searle, S., Schmutz, J., Grimwood, J., Dickson, M. C., Myers, R. M., Miller, C. T., Summers, B. R., Knecht, A. K., ... Kingsley, D. M. (2012). The genomic basis of adaptive evolution in threespine sticklebacks. *Nature*, 484(7392), 55–61. <https://doi.org/10.1038/nature10944>

Kocher, T. D. (2004). Adaptive evolution and explosive speciation: The cichlid fish model. *Nature Reviews. Genetics*, 5(4), 288–298. <https://doi.org/10.1038/nrg1316>

Koehl, M. (1984). How do benthic organisms withstand moving water? *American Zoologist*, 24, 57–70.

Konings, A. (2016). *Malawi cichlids in their natural habitat* (5th ed.). Cichlid Press.

Kusche, H., Recknagel, H., Elmer, K. R., & Meyer, A. (2014). Crater lake cichlids individually specialize along the benthic-limnetic axis. *Ecology and Evolution*, 4(7), 1127–1139. <https://doi.org/10.1002/ece3.1015>

Laghari, M. Y., Lashari, P., Zhang, X., Xu, P., Narejo, N. T., Liu, Y., Mehboob, S., al-Ghanim, K., Zhang, Y., & Sun, X. (2014). Mapping QTLs for swimming ability related traits in *Cyprinus carpio* L. *Marine Biotechnology (New York, N.Y.)*, 16(6), 629–637. <https://doi.org/10.1007/s10126-014-9578-8>

Larouche, O., Benton, B., Corn, K. A., Friedman, S. T., Gross, D., Iwan, M., & Price, S. A. (2020). Reef-associated fishes have more maneuverable body shapes at a macroevolutionary scale. *Coral Reefs*, 39, 1427–1439.

Law, C. J. (2019). Evolutionary shifts in extant mustelid (Mustelidae: Carnivora) cranial shape, body size and body shape coincide with the mid-Miocene climate transition. *Biology Letters*, 15(5), 20190155. <https://doi.org/10.1098/rsbl.2019.0155>

Law, C. J. (2021). Evolutionary and morphological patterns underlying carnivoran body shape diversity. *Evolution*, 75(2), 365–375. <https://doi.org/10.1111/evo.14143>

Liu, J., Shikano, T., Leinonen, T., Cano, J. M., Li, M. H., & Merila, J. (2014). Identification of major and minor QTL for ecologically important morphological traits in three-spined sticklebacks (*Gasterosteus aculeatus*). *G3 (Bethesda)*, 4(4), 595–604. <https://doi.org/10.1534/g3.114.010389>

Losos, J. (2009). *Lizards in an evolutionary tree: Ecology and adaptive radiation of anoles*. University of California Press.

Malinsky, M., Svardal, H., Tyers, A. M., Miska, E. A., Genner, M. J., Turner, G. F., & Durbin, R. (2018). Whole-genome sequences of Malawi cichlids reveal multiple radiations interconnected by gene flow. *Nature Ecology Evolution*, 2(12), 1940–1955. <https://doi.org/10.1038/s41559-018-0717-x>

Melo, D., Porto, A., Cheverud, J. M., & Marroig, G. (2016). Modularity: Genes, development and evolution. *Annual Review of Ecology, Evolution, and Systematics*, 47, 463–486. <https://doi.org/10.1146/annurev-ecolsys-121415-032409>

Meyers, P. J., & Belk, M. C. (2014). Shape variation in a benthic stream fish across flow regimes. *Hydrobiologia*, 738, 147–154.

Miller, C. T., Glazer, A. M., Summers, B. R., Blackman, B. K., Norman, A. R., Shapiro, M. D., Cole, B. L., Peichel, C. L., Schlüter, D., & Kingsley, D. M. (2014). Modular skeletal evolution in sticklebacks is controlled by additive and clustered quantitative trait loci. *Genetics*, 197(1), 405–420. <https://doi.org/10.1534/genetics.114.162420>

Musich, M., Indermaur, A., & Salzburger, W. (2012). Convergent evolution within an adaptive radiation of cichlid fishes. *Current Biology*, 22(24), 2362–2368. <https://doi.org/10.1016/j.cub.2012.10.048>

Navon, D., Olearczyk, N., & Albertson, R. C. (2017). Genetic and developmental basis for fin shape variation in African cichlid fishes. *Molecular Ecology*, 26(1), 291–303. <https://doi.org/10.1111/mec.13905>

Nguyen, N. T. T., Vincens, P., Dufayard, J. F., Roest Crollius, H., & Louis, A. (2022). Genomicus in 2022: Comparative tools for thousands of genomes and reconstructed ancestors. *Nucleic Acids Research*, 50(D1), D1025–D1031. <https://doi.org/10.1093/nar/gkab1091>

Peterson, E. N., Cline, M. E., Moore, E. C., Roberts, N. B., & Roberts, R. B. (2017). Genetic sex determination in *Astatotilapia calliptera*, a prototype species for the Lake Malawi cichlid radiation. *Naturwissenschaften*, 104(5–6), 41. <https://doi.org/10.1007/s00114-017-1462-8>

Pigliucci, M., & Muller, G. B. (2010). *Evolution, the extended synthesis*. MIT Press.

Powder, K. E. (2020). QTL analysis in fishes. In X. M. Shi (Ed.), *eQTL analysis*. Springer.

Powder, K. E., & Albertson, R. C. (2016). Cichlid fishes as a model to understand normal and clinical craniofacial variation. *Developmental Biology*, 415(2), 338–346. <https://doi.org/10.1016/j.ydbio.2015.12.018>

Price, S. A., Friedman, S. T., Corn, K. A., Martinez, C. M., Larouche, O., & Wainwright, P. C. (2019). Building a body shape Morphospace of Teleostean fishes. *Integrative and Comparative Biology*, 59(3), 716–730. <https://doi.org/10.1093/icb/icz115>

Raffini, F., Schneider, R. F., Franchini, P., Kautt, A. F., & Meyer, A. (2020). Diving into divergence: Differentiation in swimming performances, physiology and gene expression between locally-adapted sympatric cichlid fishes. *Molecular Ecology*, 29(7), 1219–1234. <https://doi.org/10.1111/mec.15304>

Ribeiro, E., Davis, A. M., Rivero-Vega, R. A., Orti, G., & Betancur, R. R. (2018). Post-cretaceous bursts of evolution along the benthic-pelagic axis in marine fishes. *Proceedings of the Biological Sciences*, 285(1893), 20182010. <https://doi.org/10.1098/rspb.2018.2010>

Roberts, R. B., Hu, Y., Albertson, R. C., & Kocher, T. D. (2011). Craniofacial divergence and ongoing adaptation via the hedgehog pathway. *Proceedings of the National Academy of Sciences of the United States of America*, 108(32), 13194–13199. <https://doi.org/10.1073/pnas.1018456108>

Roberts, R. B., Ser, J. R., & Kocher, T. D. (2009). Sexual conflict resolved by invasion of a novel sex determiner in Lake Malawi cichlid fishes. *Science*, 326(5955), 998–1001. <https://doi.org/10.1126/science.1174705>

Robinson, B., & Wilson, D. (1994). Character release and displacement in fishes: A neglected literature. *The American Naturalist*, 144(4), 596–627.

Roesti, M., Kueng, B., Moser, D., & Berner, D. (2015). The genomics of ecological vicariance in threespine stickleback fish. *Nature Communications*, 6, 8767. <https://doi.org/10.1038/ncomms9767>

Rogers, S. M., & Jamniczky, H. A. (2014). The shape of things to come in the study of the origin of species? *Molecular Ecology*, 23, 1650–1652.

Rogers, S. M., Tamkee, P., Summers, B., Balabahadra, S., Marks, M., Kingsley, D. M., & Schlüter, D. (2012). Genetic signature of adaptive peak shift in threespine stickleback. *Evolution*, 66(8), 2439–2450. <https://doi.org/10.1111/j.1558-5646.2012.01622.x>

Ruber, L., & Adams, D. (2001). Evolutionary convergence of body shape and trophic morphology in cichlids from Lake Tanganyika. *Journal of Evolutionary Biology*, 14(2), 325–332.

Ruff, C. (1991). Climate and body shape in hominid evolution. *Journal of Human Evolution*, 21(2), 81–105.

Schlüter, D. (1996). Ecological causes of adaptive radiation. *The American Naturalist*, 148, S40–S64.

Schlüter, D. (2000). *The ecology of adaptive radiation*. Oxford University Press.

Schlüter, D., & McPhail, J. (1992). Ecological character displacement and speciation in sticklebacks. *The American Naturalist*, 140, 85–108. <https://doi.org/10.1086/285404>

Ser, J. R., Roberts, R. B., & Kocher, T. D. (2010). Multiple interacting loci control sex determination in Lake Malawi cichlid fish. *Evolution*, 64(2), 486–501. <https://doi.org/10.1111/j.1558-5646.2009.00871.x>

Smith, A., Nelson-Maney, N., Parsons, K. J., Cooper, W., & Albertson, R. C. (2015). Body shape evolution in sunfishes: Divergent paths to accelerated rates of speciation in the Centrarchidae. *Evolutionary Biology*, 42, 283–295.

Streelman, J. T., & Danley, P. (2003). The stages of vertebrate evolutionary radiation. *Trends in Ecology & Evolution*, 18(3), 126–131.

Svardal, H., Quah, F. X., Malinsky, M., Ngatunga, B. P., Miska, E. A., Salzburger, W., Genner, M. J., Turner, G. F., & Durbin, R. (2020). Ancestral hybridization facilitated species diversification in the Lake Malawi cichlid fish adaptive radiation. *Molecular Biology and Evolution*, 37(4), 1100–1113. <https://doi.org/10.1093/molbev/msz294>

Wagner, G. P., Pavlicev, M., & Cheverud, J. M. (2007). The road to modularity. *Nature Reviews. Genetics*, 8(12), 921–931. <https://doi.org/10.1038/nrg2267>

Walker, J. A. (1997). Ecological morphology of lacustrine threespine stickleback *Gasterosteus aculeatus* (Gasterosteidae) body shape. *Biological Journal of the Linnean Society*, 61, 3–59.

Ward, A. B., & Mehta, R. S. (2010). Axial elongation in fishes: Using morphological approaches to elucidate developmental mechanisms in studying body shape. *Integrative and Comparative Biology*, 50(6), 1106–1119. <https://doi.org/10.1093/icb/icq029>

Webb, P. (1982). Locomotor patterns in the evolution of actinopterygian fishes. *American Zoologist*, 22, 329–342.

Webb, P. (1984). Body form, locomotion and foraging in aquatic vertebrates. *American Zoologist*, 24, 107–120.

Wiens, J., & Slingluff, J. (2001). How lizards turn into snakes: A phylogenetic analysis of body-form evolution in anguid lizards. *Evolution*, 55(11), 2303–2318.

Willacker, J. J., Von Hippel, F. A., Wilton, P. R., & Walton, K. M. (2010). Classification of threespine stickleback along the benthic-limnetic axis. *Biological Journal of the Linnean Society*, 101, 595–608.

Williams, T. M., & Carroll, S. B. (2009). Genetic and molecular insights into the development and evolution of sexual dimorphism. *Nature Reviews. Genetics*, 10(11), 797–804. <https://doi.org/10.1038/nrg2687>

Yang, J., Guo, B., Shikano, T., Liu, X., & Merila, J. (2016). Quantitative trait locus analysis of body shape divergence in nine-spined sticklebacks based on high-density SNP-panel. *Scientific Reports*, 6, 26632. <https://doi.org/10.1038/srep26632>

SUPPORTING INFORMATION

Additional supporting information can be found online in the Supporting Information section at the end of this article.

How to cite this article: DeLorenzo, L., Mathews, D., Brandon, A. A., Joglekar, M., Carmona Baez, A., Moore, E. C., Ciccotto, P. J., Roberts, N. B., Roberts, R. B., & Powder, K. E. (2023). Genetic basis of ecologically relevant body shape variation among four genera of cichlid fishes. *Molecular Ecology*, 32, 3975–3988. <https://doi.org/10.1111/mec.16977>